The Anatomical Record

MULTIPLE SOURCES OF SERTOLI CELLS AND TWO SERTOLI PHENOTYPES IN THE ADULT ELASMOBRANCH TESTIS: INSIGHT FROM TWO SPECIES BELONGING TO DIFFERENT ORDERS

Journal:	*Anatomical Record*
Manuscript ID	AR-18-0214.R1
Wiley - Manuscript type:	Full Length Article
Date Submitted by the Author:	n/a
Complete List of Authors:	McClusky, Leon; University of Tromsø – The Arctic University of Norway, Department of Health and Care
Keywords:	stromal cells, collecting duct, PCNA immunohistochemistry, Sertoli cells, Sertoli phenotypes

MULTIPLE SOURCES OF SERTOLI CELLS AND TWO SERTOLI PHENOTYPES IN THE ADULT ELASMOBRANCH TESTIS: INSIGHT FROM TWO SPECIES BELONGING TO DIFFERENT ORDERS

Leon Mendel McClusky

Department of Health & Care, Faculty of Health Sciences, University of Tromsø, Campus Narvik, Norway

Corresponding author:

Leon M. McClusky, PhD

Tel: +4776966239

Email: leonmcclusky@yahoo.com

Running header: Cyst – duct transition as a source of two types of Sertoli cells

Keywords: stromal cells, collecting duct, PCNA immunohistochemistry, niche region, Sertoli cells

ABSTRACT

Findings presented here for the chondrichthyans *Prionace glauca* and *Isurus oxyrinchus*, show that the assembly of the spermatocyst and collecting duct are seamlessly connected developmental phenomena. Both the cyst's somatic cell component (i.e. Sertoli cells, SCs) and the duct's constituent cells derive from a common precursor cell type (typically a large oblong cell) found among the A-spermatogonia in the folliculogenic region. Novel findings show that the co-developing collecting duct serves as a source of either normal-looking or basophilic atypical SCs (aSCs), depending on whether the duct – cyst transition remains mitotically active and open, or is sealed off from the cyst. The aSCs arise from accumulating slender basophilic cells at the duct – cyst interface after which the newly formed cyst is also sealed. Quantitative analysis of the latter in *P. glauca* revealed a correlation between the appearance of this aSC in immature cysts and the degenerated testicular condition that reveals a gradient of multinucleate cell (MNC) death among preferably mature spermatogonial cysts. Findings seem to implicate these aSCs in the life – death balance in mature spermatogonial cohorts downstream in the spermatogenic sequence, rather than in their cysts of origin that exhibit low incidences of apoptosis. Photomicrographs of developing spermatogonial cysts showing several aSCs interspersed among cytoplasmically-linked spermatogonia that are proliferating or have died, seem to suggest that these small SCs maybe involved in confining MNC death to a given cyst region under conditions of subthreshold levels of apoptosis such as to ensure cyst recovery in immature spermatogonial cysts.

INTRODUCTION

Germ cells develop into spermatozoa while engaged in a physical, intimate relationship with the Sertoli cell, the only supporting somatic cell found in the germinal compartment together with the germ cells. The orderly developmental advance of the various germ cell stages that are enwrapped at specific levels in the tree-like cell body of the Sertoli cells that line the walls of the well-studied mammalian spermatogenic tubules (Hess and Franca, 2005), have been analogously compared to the conveyor belt of a motor vehicle assembly plant (Sharpe, 1994). In the higher vertebrate testis, new germ cell generations, including the undifferentiated (type A) spermatogonia, are nurtured in the Sertoli cell's basal portions while earlier generations (spermatocytes and maturing spermatids) are still enwrapped in the supporting cell's middle and apical portions.

Each germ cell stage is, however, engaged in a physically and functionally unique relationship with the Sertoli cell. Classic studies on the laboratory rodent testis surprisingly found that the numerical ratio of type A spermatogonia to Sertoli cells may be a limiting factor (Huckins, 1978) due to significant rates of degeneration (now known as apoptosis) observed among the various generations of cycling spermatogonia in normal rats. How the Sertoli cell morphologically adapts and manages both cycling and dying spermatogonia simultaneously in vivo, is poorly understood, particularly since phagocytic removal of the dead cells must be concurrent with stimulatory signaling to the other dividing members of the same spermatogonial cohort. Asynchronous development in a single germ cell cohort is known to occur during normal spermatogenesis in higher (Miething, 2010) and lower

(McClusky, 2012) vertebrates, and even between two clone members still connected to each other via an intercellular bridge (Miething, 2010).

These and other fundamental questions have spawned interest in the study of spermatogonial kinetics in lower vertebrates (e.g. cartilaginous and bony fishes, and amphibians) that have a simpler testicular organization and lack permanent Sertoli cells. In the testes of these vertebrates, the (1) Sertoli cell embarks on a program of proliferation and differentiation simultaneously with the germ cells under its care, and (2) each germ cell cohort (i.e. stage) is found together with its own complement of Sertoli cells in anatomically discrete, spherical follicle-like units, termed spermatocysts (Callard, 1991). These features render these testes suitable for correlating Sertoli cell stage, morphology and cell kinetics with a specific stage of germ cell development (Dobson and Dodd, 1977b; Kobayashi and Iwasawa, 1992; McClusky, 2005; Loppion et al., 2008).

Routine histological examination of a single testicular cross-section of some elasmobranch species shows cysts arranged in a maturational order between the immature and mature poles of the testis. Sertoli cell nuclei gradually assume a perilumenar position in the developing spermatogonial cyst, followed eventually by their migration to the cyst periphery. The latter behavioral change marks the conclusion of the period of multiple spermatogonial divisions. Withdrawal of pituitary support in another dogfish species (*Scyliorhinus canicula*) caused massive spermatogonial degeneration in preferentially the cyst stage in which Sertoli cell nuclei were engaged in the lumen-to-periphery migration, but never in the adjacent spermatocyte cysts (Dobson and Dodd, 1977). The latter authors found that the accompanying Sertoli cells remained completely unaffected and phagocytized the degenerated

spermatogonia, developments that culminated in rows of flattened Sertoli cell-only cysts that manifested as a zone of degeneration. Similar naturally appearing zones of degeneration, known now to be massive waves of apoptosis, have since been reported in a defined area of the premeiotic region of the testis of seasonal elasmobranch species such as *Squalus acanthias* (McClusky, 2005) and *Prionace glauca* (McClusky, 2013). Moreover, some developing spermatogonial cysts with scattered loci of germ cell death may yet recover from the earlier graded onset of apoptosis as such cysts simultaneously displayed mitotic and apoptotic activity in different parts of the cysts as well as between neighboring spermatogonia (McClusky, 2012, 2013), all of which confirms the asynchrony in the cell kinetics of a single cytoplasmically linked spermatogonial clone. The latter, together with observed apoptosis resistance of newly assembled and immature spermatogonial cysts in these species allude to the existence of a putative cyst-intrinsic mechanism that may regulate the life-death balance in the germ cell clone (McClusky, 2012), with the associated Sertoli cells in the cyst postulated as the most probable source of such regulation. The discovery, in the spiny dogfish (McClusky, 2005) and an amphibian (Sasso-Cerri et al., 2006) of small atypical Sertoli cells whose nuclei assume a crescent shaped position only around the dying germ cell clone members may be one example of Sertoli cell involvement in germ cell clone asynchronous development.

A major aim of this paper was to further establish whether the above observations pertain to specific morphological changes of one member of the cyst's complement of Sertoli cells or whether it involves an entirely different Sertoli cell phenotype that arose earlier at the onset of spermatocyst assembly or even during pre-spermatogenesis. The latter rationale is related to observations of pre-spermatogenesis at the immature pole of testis in some species of slender to fusiform cells positioned in a crescent shape manner around the elasmobranch's type A

spermatogonia (Dobson and Dodd, 1977, Parsons and Grier, 1992; Loppion et al., 2008). These fusiform supporting cells, the future Sertoli cells, are rarely mitotically active or immunoreactive to a conserved marker of cell proliferation, namely proliferating cell nuclear antigen (PCNA) (McClusky, 2005, Loppion et al., 2008). A secondary aim of this study was to compare and contrast above the observations in the testes of two elasmobranch species from different orders of the Chondricthyes due to the different anatomical locations of the sites of origins of the follicle-like cysts, called here the folliculogenic regions.

MATERIALS AND METHODS

Animals

The tissues used in the present study were harvested from sexually mature, moribund specimens of two well-known pelagic species landed by sports anglers at fishing tournaments held over the early and late summer months at various sites along the northeast US coast, namely Montauk (NY) and Martha's Vineyard (MA). The specimens sampled comprised four shortfin mako sharks (*Isurus oxyrinchus* Rafinesque 1810, Order Lamniformes, Family Lamnidae, 67.8 kg – 90.3 kg; 191 – 209 cm fork length) and 10 blue sharks (*Prionace glauca* Linnaeus 1758, Order Carcharhiniformes, Family Carcharhinidae) selected from a larger sample (n=19; 67.3 – 120 kg; 213 – 262 cm fork-length) as these contained the testicular regions of interest for this study. Animal handling and dissection procedures were performed under the auspices and ethical approval of the National Oceanic and Atmospheric Administration Fisheries Service, Narragansett (RI) and its attending fisheries scientists who catalogued all landed species as part of their Apex Predators Program.

Tissue preparation and immunohistochemistry

One to two representative cross-sections (5 – 7 mm) were obtained from both testes and fixed immediately in 10% buffered elasmobranch formalin (Prieur et al., 1976) for 24-48 hours followed by storage temporarily in 70% ethanol until they were embedded in paraffin wax. Paraffin sections of 4-5 μm thickness were generated and collected on silicane-coated glass slides, dried for 30 min at 60 °C, deparaffinized and rehydrated stepwise through a graded ethanol series prior to routine histological examination with Gills II hematoxylin and eosin staining and immunohistochemistry.

The immunohistochemical protocol employed an antibody to a conserved cell cycle marker, namely proliferating cell nuclear antigen (PCNA). The use of this classical marker of proliferating spermatogonia has been optimized for elasmobranch tissues (McClusky, 2005; Borucinska et al., 2008) and previously employed as a tool to differentiate between alternatively cycling and quiescent elasmobranch spermatogonia and their Sertoli cells in immature spermatocysts (McClusky, 2005, 2013).

Hydrated tissue sections were exposed to the PC10 anti-PCNA (mouse monoclonal antibody to a recombinant mouse PCNA comprising amino acids 112-12, Calbiochem, San Diego, CA) as part of a previous study on neoplastic tissues in elasmobranchs (Borucinska et al., 2008). Briefly, endogenous peroxidase activity was quenched by treating sections in darkness with 3% hydrogen peroxide. Following a rinse in distilled water, sections were

subjected to an antigen retrieval procedure, which entailed incubation for 10 min in "Retrieve-all" pH 8.0 (Signet Laboratories, Dedham, MA, USA) in a steamer bath, followed by 10 min 'cool down' at RT. After two washes in diluted Cadenza buffer wash (Thermo Electron Corp., Waltham, MA, USA) which was also used in all subsequent washes, sections were then incubated with Omnitags protein blocking solution (Thermo Electron Corp., Waltham, MA, USA) for 5-10 min at RT to reduce non-specific binding, and then overnight at RT with anti-PCNA PC10 (a mouse monoclonal antibody derived against a recombinant mouse PCNA consisting of amino acids 112-121; Calbiochem, San Diego, CA, USA) at final concentration 0.001 μg/μL.

After three buffer washes, sections were incubated at 1:40 dilution in biotinylated anti-mouse secondary antibody (Thermo Electron Corp., Waltham, MA, USA) for 30 min at RT. Following three buffer washes, sections were incubated with the Vectastain streptavidin-peroxidase complex (Vector Laboratories, Burlingame, CA, USA) for a further 20 min at RT. The antigen was finally detected by treating the sections with Vector Nova Red substrate kit (Vector Laboratories, Burlingame, CA, USA) for 10 min, counterstained with Shandon Gill 2 hematoxylin (Thermo Electron Corp., Waltham, MA, USA), dehydrated, cleared and mounted with Permount (Fisher, Fairlawn, NJ, USA). Negative controls were generated by incubating sections with optimally diluted mouse isotype antibody (Thermo Electron Corp., Waltham, MA, USA).

Microscopy

Sections were viewed, analysed and the regions of interest photographed with Leica DMLS bright field microscope fitted with Visicam 5.0 digital camera (VWR, Belgium).

Analyses focused on the folliculogenic region (the site of origin of the cysts) and the testicular region with the next stage of spermatogenic development, namely the germinal zone (GZ) that housed the newly assembled cysts. In all elasmobranchs, the developmental advance and growth of spermatogonial cysts manifest histologically as the gradual rearrangement of the cyst's cellular contents with respect to the Sertoli cell nuclei and the development of a cyst lumen. Thus, a cyst in which the Sertoli cell nuclei and those of the B-spermatogonia are arranged in no particular order around the cyst lumen may be classified as *non-patterned*, which is distinct from a *patterned* spermatogonial cyst with its characteristic perilumenar Sertoli cell nuclei and peripherally located B-spermatogonia.

Quantitative analysis of non-patterned spermatogonial cysts seen in a cross-section of the testis of *P. glauca* was as described previously (McClusky, 2013). All non-patterned cysts in the GZ that intersected or were contiguous to three lines radiating from the folliculogenic region were counted and classified according to the type of immigrating duct cell at the cyst opening.

Statistical analysis

Quantitative analyses were raw percentage data expressed as the mean percentage ± S.E.M of spermatocysts (Fig. 7) analysed by one-way analysis of variance (ANOVA) using InStat version 2.03 (GraphPad Software, San Diego, CA). The Student Newman-Keuls multiple-comparison test was used to identify mean percentages that differed significantly ($P<0.001$).

RESULTS

Although both are sausage-shaped, the internal organization of the testes of *P. glauca* and *I. oxyrinchus* are very different (Fig. 1). In *P. glauca*, successively maturing spermatocysts radiate from a macroscopically discernible whitish fibrous germinal ridge (GR) that runs the length of testis on its midventral surface (i.e. the so-called diametric testis type). In *I. oxyrinchus*, however, each one of the several longitudinally oriented lobes that comprise the testis possesses its own set of concentric layers of maturing cysts that have their origin in a folliculogenic region located in the middle of each lobe (i.e. the so-called radial testis type).

In *P. glauca*, the undifferentiated (type A) spermatogonia are found in germinal nests. The latter are scattered throughout the length of the stroma-rich GR (Fig. 2). When tissue sections are surveyed after PCNA immunohistochemistry, the nest reveals variably immunostained A-spermatogonia, whose nuclei typically show a light to dark brown speckled architecture (Fig. 2). The germinal nest owes its distinctive histology to immunostained fusiform somatic cells positioned in a crescent shaped manner around the type A spermatogonium with its voluminous cytoplasm (Fig. 2). The nest of *P. glauca* also reveals two other somatic cell types, namely PCNA-positive small ovoid to fusiform cells and PCNA-negative large irregular shaped to oblong cells. Some nests show the small ovoid to fusiform cells to be arranged in parallel rows among the A-spermatogonia, clearly indicating the early stages of the assembly of a collecting duct in the nest (Fig. 2).

Some areas of the GR do not display the iconic germinal nests but instead reveal a rearrangement of the soma – germ line relationships due to the large irregular shaped to oblong cells that aggregate both around the nest and amongst preferably single A-spermatogonia that visibly lack crescent shape-positioned fusiform cells that delimit the boundaries of their cytoplasm (Fig. 3A). In what appears to be the further development of the latter, the spermatogonia are seen scattered in branching cords that consist of the large irregular shaped to oblong stromal cells (Fig. 3B). The tips of the cords are delineated by single spermatogonia, from which large irregular shaped to oblong stromal cells extend in a row that joins with others to form a thicker row of oblong stromal cells that extends in the direction of the next testicular region, namely the germinal zone (Fig. 3B). These branching cords ultimately give rise to long collecting ducts, herewith proposed as the primary collecting ducts (Fig. 3C), that are histologically more prominent than the developing duct system in the germinal nest.

The histology of the germinal zone (GZ) is decidedly more parenchymal than stromal and comprises a mix of single large oblong stromal-derived cells and their tubular formations, and single immunostained spermatogonia, many of which display intense homogeneously brown immunostaining. The location of the assembly of the cysts is seemingly confined to the sites where the large oblong stromal-derived cells are arranged as branching cords (Fig. 3B), all of which results in the early testicular parenchyma initially appearing more tubular-like than cyst-like. The cysts are observed as open buds or sacs at the termini of the lengthening ducts (Fig. 4A). Since ducts may also develop along the length of the testis, a sac may then be easily mistaken for a cross-sectioned profile of such a duct, if it is not for the presence of a lone intensely brown immunostained spermatogonium among the large Sertoli cells that are morphologically identical to the duct cells (Fig. 4A). The presence, therefore, of a single

spermatogonium in an open ring of almost only Sertoli cells that resemble duct cells and the arrangement of the large oblong stromal-derived cells as cords (Fig. 3B) may imply that the large oblong stromal-derived cells are arranged in a ring-like fashion on either side of the spermatogonium, with the stromal-derived cells laid down in parallel rows that extend from the two ends of the ring (i.e. the cyst). Fig. 4B shows the incorporation of large oblong stromal-derived cells from aggregations close to the growing duct. The latter is in turn connected to the cysts via a neck region that consists of ovoid to elongated duct cells. The duct cells nearest to the cyst opening gradually transform first into ovoid and then into increasingly basophilic elongated cells that ultimately seal the lumen of the cyst from that of the duct (Fig. 4B, C), with the latter phenomena observed only in some newly formed cysts (see below). The Sertoli : germ cell ratio of newly formed cysts varies greatly, but Sertoli cell-dominating cysts are prevalent in the GZ, as evident from negative control staining that highlights the two distinctively basophilic spermatogonia among the large oblong Sertoli cells in the cyst (Fig. 4D).

Developing *P. glauca* spermatogonial cysts that house Sertoli cells with bulky oblong nuclei show two types of duct – cyst transitions. The one type of transition shows a series of phenomena, the beginnings which are already evident as shown in Fig. 4C, and that proceed with the sealing of the cyst compartment by an expanding population of very slender basophilic cells (Fig. 5A) that ultimately give rise to a dark atypical Sertoli cell in some cysts (Fig. 5B, C). The site of contact between the duct and cyst shows the generation of initially very slender, highly basophilic cells that undergo a gradual transformation simultaneously as their long axes are increasingly reoriented perpendicular to the cyst periphery (Fig. 5B, C). The latter cells aggregate and partially curve around the spermatogonia on their luminal side (Fig. 5C). Blue bands on the cyst periphery, irrespective of their orientation, readily disclose

the presence of these transforming basophilic cells in small GZ cysts during a cursory examination of a PCNA immunohistochemically stained slide preparation. The latter developments are commonly seen in cysts that house one or two intense homogeneously brown immunostained spermatogonia, or those with an increasingly translucent or foamy appearance with light brown staining. The latter appearance develops from the former (data not shown).

The second type of duct – cyst transition reveal the supplementation of the cyst's Sertoli cell population with neck duct cells of similar morphology. As shown in Fig. 5D, the mitotically active neck region of the duct is histologically distinct from the primary collecting duct that is assembled from broad oblong cells found scattered in the interstitium, and which never exhibit any signs of mitosis (Fig. 5D). The observations are inconclusive about the origins of the neck duct cells described above, but it would appear they derive from the primary collecting duct's broad oblong cells.

The neck duct cells themselves also reveal differences among newly assembled *P. glauca* cysts. Fig. 6A shows that they are distinctly elongated with pointed ends, very similar to the fusiform cells that comprise the developing duct observed within the germinal nest (see Fig. 2). Unlike that described above for cysts with large oblong Sertoli cells, the sac-like cysts affixed to the latter type of neck region are never sealed (Fig. 6A). Instead, the duct – cyst transition is a dynamic region, as revealed by duct cell mitosis that clearly contributes towards an overcrowded duct – cyst transition with the resultant displacement of such duct cells into the cyst that already houses similar shaped Sertoli cells (Fig. 6B).

Unlike the folliculogenic region of *P. glauca* that lies as a ridge on the surface of the testis, that of *I. oxyrinchus* is located in the center of each lobe and thus macroscopically indiscernible. It consists of ovoid to oblong stromal cells among which are scattered large spherical similarly uniformly immunostained type A spermatogonia (Fig. 7A). The putative pre-Sertoli cells are not readily distinguishable from the folliculogenic region's stromal cells. The periphery of the folliculogenic region reveals the ring-shaped arrangement of immunonegative stromal cells alongside a lone PCNA immunostained spermatogonium, all of which definitively identifies these structures as newly assembled cysts (Fig. 7B). The peripheral layer of the consistently PCNA immunostained spermatogonia in growing spermatogonial cysts is often incomplete due to the presence of many gaps (Figs. 7C, 8C) that result from spermatogonial cell death, the remains of which may be seen in some cysts (Fig. 7D). This contrasts with the densely packed perilumenar layer of consistently immunonegative Sertoli cell nuclei. The cyst's Sertoli cell numbers are additionally supplemented by immigrating duct cells that have noticeably cloudy nuclei (Fig. 7C), a development that attenuates with further cyst growth (Fig. 7D).

As in *P. glauca*, the duct – cyst interface in large *I. oxyrinchus* spermatogonial cysts also reveal the inward movement of slender to fusiform strongly basophilic duct cells that ultimately manifest as the dark atypical Sertoli cells (Fig. 8B). In both species, the latter atypical Sertoli cells are observed in enlarging spermatogonial cysts that contain dividing spermatogonia (Fig. 8A) and/or the remnants of cell death (Figs. 7D; 8A, B),

Not all perturbations of the life-death balance are associated with the latter Sertoli cell type, at least not as seen during the perusal of only single cross-sections of cysts whose

diameters range from 200 to 400 micrometers. The photomicrographic evidence from both species, nevertheless, appear to implicate the dark atypical Sertoli cells in the life – death balance in spermatogonial cohorts further downstream in the spermatogenic sequence, rather than in the newly formed cysts with their sparse spermatogonia.

An earlier analysis of the life-death balance in germ cell cohorts during spermatogenesis found that the large mature, rather than the small immature spermatogonial cysts of summer breeding *P. glauca* displayed a protracted two-stage form of caspase 3-dependent cell death, all of which allowed the distinction between two types of testicular conditions in these wild-caught specimens (McClusky, 2013). The latter study distinguished histologically between testes that showed extensive multinucleate cell death (MNC) in preferentially mature spermatogonial cysts, and those with vacuolated areas in the spermatogonial layers of the same cyst stages. It was concluded that Sertoli cell phagocytic clearing of the MNC germ cell corpses was the most likely explanation for the appearance of numerous vacuolated areas in the large spermatogonial and spermatocyte cysts in the testes of some the specimens that show clear evidence of an early recovery phase.

Given the ready distinction between these two cell death-associated testicular conditions, it was therefore determined to express the respective proportions of newly formed (non-patterned) cysts whose cyst openings show evidence of slender basophilic (blue) cells, and those cysts with immigrating elongated to fusiform duct cells at the cyst opening as a function of testicular condition (Fig. 9). Overall, the calculated differences, in both testicular conditions, of the proportions of non-patterned cysts exhibiting evidence of Sertoli cell supplementation, irrespective of type, were significant ($P < 0.0001$, Fig. 9). The proportion of

cysts with slender blue cells at the cyst opening was significantly ($P < 0.001$) 9-fold greater in the degenerate testicular condition than in the early recovery phase. Conversely, the proportion of cysts that in turn revealed immigrating elongated to fusiform duct cells at the cyst opening was likewise significantly ($P < 0.001$) 9-fold greater in the early recovery testicular condition than in the degenerate testis.

DISCUSSION

Findings presented here for *P. glauca* and *I. oxyrinchus* show that the spermatocyst and the collecting duct share a common origin in the folliculogenic region, as previously suggested (Callard, 1991; Grier, 1993). A novel aspect though of these findings concerns the cyst's co-developing sperm drainage duct system that also serves as an additional source of both normal looking, mitotically active, and atypical (small and dark) Sertoli cells after its assembly (i.e. after the commitment of the A-spermatogonia to the program of spermatogonial differentiation). In some newly assembled cysts and specifically those with densely populated, dynamic duct – cyst transition areas, the immigrating progeny of dividing elongated neck duct cells at the cyst-opening supplement the numbers of the cyst's normally proportioned Sertoli cells that are also dividing. Conversely, Sertoli cell-dominated newly assembled cysts whose large oblong Sertoli cells very rarely engage in mitosis are supplemented with a different, and distinctly atypical Sertoli cell that derives from developing slender basophilic duct cells at the cyst opening that simultaneously seal off the cyst compartment from the attached collecting duct. The pronounced basophilia (intense blue staining) that accompanies their transformation into Sertoli cells greatly assists in the distinction between the two types of Sertoli cell supplementation early on in spermatogenesis. Taken together, these findings suggest that the

cell kinetics of the newly formed cyst's Sertoli cells are intricately linked to the type of duct – cyst transition, namely whether it is inactive or dynamic.

During the cystic spermatogenesis of elasmobranchs, each germ cell clone develops with its own set of Sertoli cells in the cysts. Any change therefore in the numbers or morphology of the Sertoli cell can therefore be directly coupled to a given germ cell stage during a cursory survey of a cross-section. The observed differences reported here between duct – cyst transition areas that ultimately resulted in that some cysts were sealed off from the duct and others not, were unexpected findings. A consistent observation though was that the sealing of the cyst compartment was noted only in cysts dominated by large bulky oblong Sertoli cells. Moreover, the latter cysts, as a rule, housed few spermatogonia with either dark blue or intense homogeneously brown immunostained nuclei with or without translucent areas in the non-speckled nucleoplasm, all of which suggest an association between the cell cycle status of the spermatogonia and the morphology of the accompanying Sertoli cell. A cogent interpretation of the above findings may therefore benefit first from a correlative analysis (in preparation) of the proportions of cysts whose spermatogonia exhibit a given type of PCNA immunostaining and type of Sertoli cell (compare figs. 3 and 5)

The functional significance of two types of *de novo* extra-cystic supplementation of Sertoli cell numbers and the quantitative correlation of these phenomena with a given testicular condition (degenerate or early recovery) overall and in terms of seminal events in the premeiotic phase of spermatogenesis (i.e. germ cell proliferation and death) is not immediately clear. Mindful of the protracted nature of the developmental advance of the elasmobranch cysts, it is more than likely that newly assembled cysts located upstream from

more mature spermatogonial cysts in any given cross section may belong spatiotemporally to a different wave of spermatogenesis (Fig. 10), as also previously reported for *S. acanthias* (McClusky, 2005) and *P. glauca* (McClusky, 2013). One interpretation of the photomicrographic evidence presented here, and schematically illustrated in Fig. 10, may therefore be that the dark atypical Sertoli cells are likely involved in the life – death balance at a subsequent cyst stage in the spermatogenic sequence, rather than in the sealed newly formed cysts where they first appear. The evidence presented here regarding an ancient vertebrate's testis with its non-permanent Sertoli cells and extra-cystic supplementation of Sertoli cell numbers in the cyst (germinal) compartment may testify of an ancestral-like mechanism of adjusting the Sertoli : germ cell ratio in a given cyst (germ cell clone) in advance of cell kinetic events at a later stage of cyst development,0.

Quantitative analyses of the apoptosis gradient in the expansive premeiotic (PrM) regions of *Squalus* (McClusky, 2012) and *P. glauca* (McClusky, 2011, 2013) noted the low incidence of multinucleate cell (MNC) corpses among immature PrM cysts, and their preponderance among mature PrM cysts. In both elasmobranchs, some developing PrM cysts that display a scattering of MNC death corpses may yet recover from the earlier graded onset of cell death since such cysts simultaneously display mitotic and apoptotic activity in different parts of the cysts as well as between neighboring spermatogonia (McClusky, 2012, 2013). It is plausible that the statistically and highly significant quantitative correlation revealed here between the proportion of newly assembled cysts with the small dark Sertoli cells and the degenerate testicular condition may well relate to a putative role of small atypical Sertoli cells in limiting the spread of MNC death to a confined area in cysts engaged in the nonpatterned → patterned transition simultaneously as they promote compensatory spermatogonial mitosis (see Fig. 7A)

under conditions of subthreshold levels of apoptosis that ultimately favor cyst recovery (Fig. 10).

It needs to be emphasized as well that not all overtly manifested perturbations of the life – death balance in growing spermatogonial clones are associated with the small dark Sertoli cell type, a possible explanation being that the phenomenon might very well be underestimated when analyzing single cross-sections of large spermatogonial cysts whose diameters may range from 200 to 400 µm. The findings presented here of small atypical Sertoli cells in cysts with evidence of cell death are, nevertheless, consistent with observations in *Squalus* (McClusky, 2005) and in an amphibian species (Sasso-Cerri et al., 2006) of distinctly slender Sertoli cells that partially curved around apoptotic germ cells. However, the origins of the latter observed atypical Sertoli cells were not discussed in these two studies.

Comparable data in other vertebrates are, however, scarce. Mechanistic investigations between the rat Sertoli cell and germ cell deletion interestingly found that experimentally forced contraction of the Sertoli cell body (to a smaller size) induced germ cell sloughing *in vivo* (Nakai et al., 1995), and activated the apoptotic program in the spermatogonial clone it nurtured *in vitro* (Tres and Kierszenbaum, 1999). Also, a reduction in the Sertoli cell's cytoplasmic volume and concomitant increased electron density (when viewed ultrastructurally) was associated with rapid live germ cell desquamation, a cell death phenomenon that preceded the fully regressed inactive testis in the seasonally reproducing Iberian mole (Dadhich et al., 2013). All in all, these findings suggest that a change in the Sertoli cell to a smaller size in response to the need to delete germ cells from the germinal compartment and/or restore tissue homeostasis, maybe a conserved trait of this indispensable

vertebrate testicular cell. It is speculated that the permanent higher vertebrate Sertoli cell's germ cell stage-related plasticity and flexibility (Franca et al., 2016) may be indicative an evolutionary past of separate Sertoli cell phenotypes, each with a morphological versatility that was consistent with the germinal clone it accompanied in the spermatocyst (Callard, 1991; Yoshida, 2016).

ACKNOWLEDGEMENTS

This study was funded, in part, by support from the Research Council of Norway. The author is greatly indebted to Dr. J Borucinska of the Department of Biology, University of Hartford, and Dr. D Wood of the Department of Pathobiology and Veterinary Sciences, University of Connecticut, CT, USA for supplying the tissues and the PCNA immunohistochemistry work.

LITERATURE CITED

Borucinska JD, Schmidt B, Tolisano J, Woodward D. 2008. Molecular markers of cancer in cartilaginous fish: immunocytochemical study of PCNA, p-53, myc and ras expression in neoplastic and hyperplastic tissues from free ranging blue sharks, *Prionace glauca* (L.). J Fish Dis 31:107-115.

Callard GV. 1991. Spermatogenesis. In: Pang PKT, Schreibman, M. P., editor. Vertebrate Endocrinology: Fundamentals and Biomedical Implications. New York: Academic Press. p 303-342.

Callard GV, Betka M, Jorgensen JC. 1994. Stage-related functions of Sertoli cells: Lessons from lower vertebrates. In: Bartke A., editor. Function of Somatic Cells in the Testis. New York, NY: Springer New York. p 27-54.

Dadhich RK, Barrionuevo FJ, Real FM, Lupiañez DG, Ortega E, Burgos M, Jiménez R. 2013. Identification of live germ-cell desquamation as a major mechanism of seasonal testis regression in mammals: A study in the Iberian mole (*Talpa occidentalis*). Biol Reprod 88:101-112.

Dobson S, Dodd JM. 1977. Endocrine control of the testis in the dogfish *Scyliorhinus canicula* L. II. Histological and ultrastructural changes in the testis after partial hypophysectomy (ventral lobectomy). Gen Comp Endocrinol 32:53-71.

Franca LR, Hess RA, Dufour JM, Hofmann MC, Griswold MD. 2016. The Sertoli cell: one hundred fifty years of beauty and plasticity. Andrology 4:189-212.

Grier HJ. 1993. Comparative organization of Sertoli cells including the Sertoli cell barrier. In: Russell LD, Griswold MD, editors. The Sertoli Cell. Clearwater, Florida: Cache River Press. p 703 - 739.

Hess RA, França LR. 2005. Structure of the Sertoli Cell. In: Skinner MK, Griswold MD, editors. Sertoli Cell Biology. San Diego: Academic Press. p 19-40.

Huckins C. 1978. The morphology and kinetics of spermatogonial degeneration in normal adult rats: an analysis using a simplified classification of the germinal epithelium. Anat Rec 190:905-926.

Kobayashi T, Iwasawa H. 1992. Timing of proliferation of spermatogonia and spermatogonium-supporting Sertoli cells in the newt *Cynops pyrrhogaster*. Biomed Res 13:167-172.

Loppion G, Crespel A, Martinez A-S, Auvray P, Sourdaine P. 2008. Study of the potential spermatogonial stem cell compartment in dogfish testis, *Scyliorhinus canicula* L. Cell Tissue Res 332:533-542.

McClusky LM. 2005. Stage and season effects on cell cycle and apoptotic activities of germ cells and Sertoli cells during spermatogenesis in the spiny dogfish (*Squalus acanthias*). Reproduction 129:89-102.

McClusky LM. 2011. Testicular degeneration during spermatogenesis in the blue shark, *Prionace glauca*: nonconformity with expression as seen in the diametric testes of other carcharhinids. J Morphol 272:938-948.

McClusky LM. 2012. Coordination of spermatogenic processes in the testis: lessons from cystic spermatogenesis. Cell Tissue Res 349:703-715.

McClusky LM. 2013. The caspase-dependent apoptosis gradient in the testis of the blue shark, *Prionace glauca*. Reproduction 145:297-310.

Miething A. 2010. Local desynchronization of cellular development within mammalian germ cell clones. Ann Anat 192:247-250.

Nakai M, Hess RA, Netsu J, Nasu T. 1995. Deformation of the rat Sertoli cell by oral administration of carbendazim (methyl 2-benzimidazole carbamate). J Androl 16:410-416.

Parsons GR, Grier HJ. 1992. Seasonal changes in shark testicular structure and spermatogenesis. J Exp Zool 261:173-184.

Prieur DJ, Fenstermacher JD, Guarino AM. 1976. A choroid plexus papilloma in an elasmobranch (*Squalus acanthias*). J Natl Cancer Inst 56:1207-1209.

Sasso-Cerri E, Cerri PS, Freymuller E, Miraglia SM. 2006. Apoptosis during the seasonal spermatogenic cycle of *Rana catesbeiana*. J Anat 209:21-29.

Sharpe RM. 1994. Regulation of spermatogenesis. In: Knobil A, Neill JD, editors. The Physiology of Reproduction, 2nd ed. New York: Raven Press. p 1363-1434.

Tres LL, Kierszenbaum AL. 1999. Cell death patterns of the rat spermatogonial cell progeny induced by sertoli cell geometric changes and Fas (CD95) agonist. Dev Dyn 214:361-371.

Yoshida S. 2016. From cyst to tubule: innovations in vertebrate spermatogenesis. WIREs Dev Biol 5:119.131.

FIGURE LEGENDS

Figure 1. A schematic illustration (not drawn to scale) that compares and contrasts the cross-sectional views of the diametric testis of *P. glauca* and the radial testis of *I. oxyrinchus*. The testicular parenchyma of the latter's testis displays a lobular organization, with each lobule consisting of its own set of sequentially maturing follicle-like cysts radiating (broken arrows) from a stroma-rich folliculogenic region (FR) in the center of the each lobule where the undifferentiated (type A) spermatogonia are located. In *P. glauca*, the latter are found in nests scattered in the white-greyish FR, that is macroscopically discernible as a germinal ridge (GR) externally along the midventral surface of the testis. A mass of lymphomyeloid tissue, known as the epigonal organ (EO) and which is the bone-marrow equivalent in elasmobranchs, is affixed to either the mature pole of the testis (e.g. in *P. glauca*) or may nearly envelop the whole testis (e.g. *I. oxyrinchus*).

Figure 2. The germinal ridge of the blue shark testis as revealed by PCNA immunohistochemistry. A germinal nest comprising large variably PCNA immunostained

type A spermatogonia (sg), and two somatic cell types, namely large PCNA-negative irregular shaped to oblong cells (filled arrows), and small immunostained ovoid to fusiform cells (open arrows). The latter's arrangement in parallel rows indicate the early stages of the assembly of a collecting duct. Immunostained fusiform somatic cells (fu) are also closely aligned to several type A spermatogonia. Bar = 20 μm.

Figure 3. Pre-spermatogenesis is associated with a rearrangement of the soma – germ line relationships in the germinal ridge (GR) of *P. glauca*. (A) Large irregular shaped to oblong stromal cells (filled arrows) aggregate around (black circled areas) and amongst small groups of A-spermatogonia (sg), some of which visibly lack an accompanying fusiform supporting cell (fu) and are instead surrounded by the former somatic cell type (filled arrows). (B) A hematoxylin and eosin-stained section showing a region of the GR and the development of branching cords comprising the large irregular shaped to oblong stromal cells (white circled area). The spermatogonia (asterisks), that are scattered along the cords also demarcate the limits of the cord branches (C) A further development shows the assembly of a decidedly thick collecting duct (cd) from the latter somatic cell type (filled arrows). Bar = 20 μm.

Figure 4. The developing testicular parenchyma in the germinal zone of adult *P. glauca* is initially more tubular-like than cyst-like. (A) The appearance of large oblong stromal-derived cells arranged in open ended rings, housing a single isolated spermatogonium (sg), at the termini of the lengthening collecting duct (cd) identify the rings as the early cysts and the oblong cells as the Sertoli cells (underlined). (B, C) Growth of the collecting ducts is also due to the incorporation of large oblong stromal cells (black filled arrows) that aggregate around the ducts. The duct cells nearest to the cyst opening become gradually ovoid to elongated

(black open arrows). The duct cells bordering on the Sertoli cells that demarcate the cyst opening are strongly basophilic slender elongated cells (arrowheads). The latter seal the cyst opening, and may take up positions among the Sertoli cells (filled arrowheads). Note the consistent absence of Sertoli cell mitotic figures. (D). A negative control section that shows a Sertoli cell-dominated cyst with a few basophilic spermatogonia (sg) and Sertoli cells that display bulky oblong nuclei (underlined). Mitotically active duct cells (white open arrows), spermatogonial mitosis (black asterisk). Bar (A, B, C) = 10 μm, D = 5 μm.

Figure 5. The two types of duct – cyst transitions observed in developing *P. glauca* spermatogonial cysts with Sertoli cells that possess large oblong nuclei (underlined, Scn). (A) A suitable plane of sectioning through a newly formed cyst shows the one type of duct – cyst transition, during which the cyst opening is sealed by slender, spindle-shaped basophilic cells (open arrows) and reinforced by large duct cells. (B) The duct – cyst interface in other cysts show the generation of extremely slender spindle-like basophilic cells (white arrowheads) that undergo a gradual transformation (black arrowheads) simultaneously as their long axes are increasingly reoriented perpendicular to the cyst periphery. (C) A tangentially sectioned cyst showing that the slender, transforming basophilic cells (black arrowheads) may aggregate in between the oblong Sertoli cell nuclei (Scn) and curve around the spermatogonia (sg) on their luminal sides, all indicative of the appearance of an atypical Sertoli cell type. *Inset*: A newly formed Sertoli cell-dominated cyst with several slender atypical Sertoli cells (black arrowheads) interspersed among the large oblong Sertoli cells. (D) In other spermatogonial cysts with large oblong Sertoli cells, such as these two patterned cysts with perilumenar Sertoli nuclei (underlined), duct cell mitotic activity (black asterisk) in the neck region and duct – cyst interface causes the displacement of duct cells (filled arrows) into the cysts. Notes that the cyst's Sertoli cell population is also experiencing a wave of mitosis. The duct neck

region is distinct from the primary collecting duct (cd) that consists of broad oblong cells (asterisk-labeled filled arrows) found scattered in the interstitium. Bar = (A, B, C) = 10 µm, D = 20 µm.

Figure 6. Some spermatogonial cysts of *P. glauca* house Sertoli cells whose nuclei have irregular, often elongated profiles and pointed ends. (A) The cyst's Sertoli cell complement (underlined) is supplemented by similar-looking duct cells (long arrows) migrating in from the neck region (ne). (B) A deeper plane of sectioning through a larger cyst reveals a dynamic duct – cyst transition area and the continued displacement of elongated duct cells into the cyst (filled arrows). Note the markedly different quality of immunostaining and architecture of the spermatogonial nuclei (sg). Duct and Sertoli cell mitoses (black and white asterisks), respectively. Bar = 10 µm.

Figure 7. The duct – cyst relationship in newly formed and growing spermatogonial cysts in *I. oxyrinchus*. (A) Large spherical and frequently PCNA-positive A-spermatogonia (white filled arrows) are seen scattered among ovoid to oblong cells (black filled arrows) that comprise the homogeneous stromal tissue in this species. (B) The ring shaped arrangement of stromal cells, some of whom are weakly PCNA immunoreactive, alongside a lone moderate to strong PCNA immunostained spermatogonium (white filled arrows) definitively identifies these structures as cysts and the stromal-like cells as the Sertoli cells (underlined). Note that the assembly of the cyst takes precedence over that of the collecting duct (black open arrows). *Inset*: Occasionally observed mitotic figures (asterisk) in an otherwise Sertoli cell-dominated (underlined) cyst are those of dividing spermatogonia. (C) The duct – cyst transition area in larger patterned spermatogonial cysts shows an accumulation of duct cells with noticeably

cloudy nuclei, some of which are displaced (arrowheads) towards the pale bulky Sertoli cell nuclei (Scn) that line the cyst lumen. (D) The inward displacement of duct cells (arrowheads) that supplement the Sertoli cell population (Scn) gradually declines with subsequent growth of the spermatogonial cyst. Note the presence of pyknotic bodies in this cyst (white open arrows) that result from spermatogonial death. Bar = 20 µm.

Figure 8. In both (A) *P. glauca* and (B, C) *I. oxyrinchus*, some developing patterned spermatogonial cysts may reveal the atypical Sertoli cell with its basophilic elongated to fusiform nucleus. (A) These atypical Sertoli cells (open arrowheads) are observed in close proximity to dividing B-spermatogonia (sg) and cell debris (white arrows). *Inset*: Such a Sertoli cell is sometimes seen tightly apposed to spermatogonia undergoing multinucleate cell death (asterisk-labelled white arrow) in mature patterned cysts further downstream in the spermatogenic sequence. (B) A comparable *I. oxyrinchus* cyst likewise shows these small dark Sertoli cells in proximity to vacuolated areas (filled arrowheads) that may or may not reveal pyknotic bodies (white arrows). Note the aggregation of the small dark Sertoli cells at the duct – cyst interface. (C) Negative control of cross section adjacent to that shown in (B). The large vacuolated area (asterisk) in the spermatogonial layer is bordered by two atypical Sertoli cells. Bar (A, B) = 10 µm, C = 20 µm.

Figure 9. Percentages of non-patterned cysts that show differences in the type of immigrating duct cell at the cyst opening, expressed as a function of testicular condition in wild-caught *P. glauca* specimens (n = 10). Values represent the mean percentage ± S.E.M non-patterned cysts analyzed by one-way ANOVA. The Student Newman-Keuls multiple comparison test

was used to identify mean percentages that differed significantly. Different letters and asterisks indicate significant differences ($P < 0.001$).

Figure 10. A schematic representation, based on previous quantitative analyses (McClusky, 2011, 2013), that sketches the putative involvement of the small atypical Sertoli cell in successive spatiotemporal changes of cyst stages (mainly spermatogonial and spermatocyte cysts) that readily reveal the onset of the wave of multinucleate cell (MNC) death and vacuolated areas in testicular cross-sections of summer-breeding *P. glauca*. Each column of cysts portrays a snapshot of the relevant spermatogonial and spermatocyte cysts found in a single cross-section of the testes from specimens whose cyst compositions were relatively similar, all of which facilitated the extrapolation of the developmental advance of these cyst stages, and the onset and progression of the wave of MNC death in the latter cyst stages (squares) forwards and backwards in time. As discussed previously (McClusky, 2013), the vacuolated appearance in indicated cyst stages is evidence of the Sertoli cell's phagocytic removal of the earlier formed MNC corpses (squares). The significant quantitative correlation between immature spermatogonial cysts that reveal the small atypical Sertoli cells and the degenerated testicular condition (wave of MNC death) reported in Fig. 9 are related to two phenomena manifested in affected cysts. The first phenomenon is the limitation of the spread of MNC wave of death in these immature spermatogonial cysts that contain some atypical Sertoli cells (i.e. a spatial effect) that in turn corresponds in time with a second phenomenon, namely the latter's normal developmental advance to the mature spermatogonial cyst stage (red-shaded area) during the early recovery or vacuolated appearance phase (i.e. a temporal effect), all of which in turn may explain the full recovery of the testis in this highly seasonal species. This rationale follows previously reported (McClusky, 2011) quantitative analyses which showed a lower and higher fraction of degenerated spermatogonial and spermatid cysts,

respectively, in the vacuolated testicular state compared to those cysts in the MNC affected testes. In other words, the effects of the wave of MNC death are evident in subsequent cyst stages in the early recovery phase, with no new degenerated phenomena arising in the recovering testis. Insets A and B show the typical PCNA immunostaining patterns of newly assembled cysts in the GZ that may either lack (A) or reveal (B) the appearance of these highly recognizable blue atypical Sertoli cells. Note that spermatogonia in these Sertoli cell-dominating cysts are characteristically either PCNA-negative (quiescent, white asterisk) or may reveal intense homogeneously or variable brown immunostaining (black asterisks).

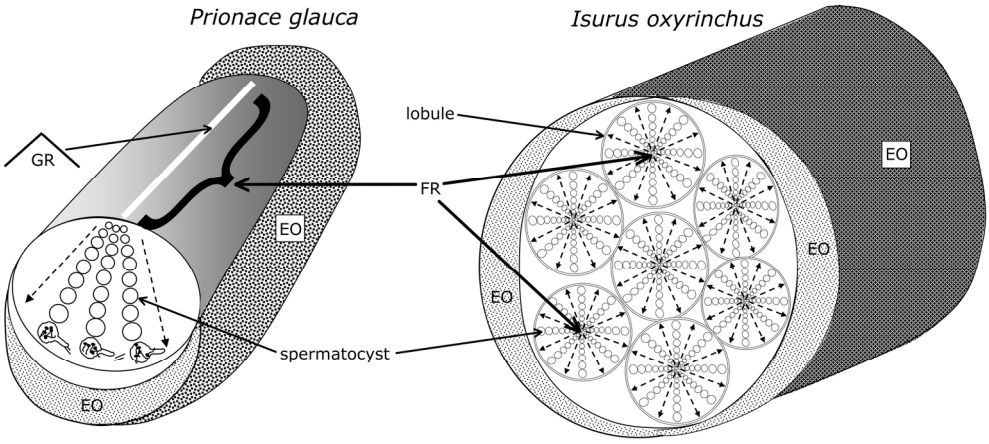

Figure 1. A schematic illustration (not drawn to scale) that compares and contrasts the cross-sectional views of the diametric testis of *P. glauca* and the radial testis of *I. oxyrinchus*. The testicular parenchyma of the latter's testis displays a lobular organization, with each lobule consisting of its own set of sequentially maturing follicle-like cysts radiating (broken arrows) from a stroma-rich folliculogenic region (FR) in the center of the each lobule where the undifferentiated (type A) spermatogonia are located. In *P. glauca*, the latter are found in nests scattered in the white-greyish FR, that is macroscopically discernible as a germinal ridge (GR) externally along the midventral surface of the testis. A mass of lymphomyeloid tissue, known as the epigonal organ (EO) and which is the bone-marrow equivalent in elasmobranchs, is affixed to either the mature pole of the testis (e.g. in *P. glauca*) or may nearly envelop the whole testis (e.g. *I. oxyrinchus*).

85x38mm (600 x 600 DPI)

Figure 2. The germinal ridge of the blue shark testis as revealed by PCNA immunohistochemistry. A germinal nest comprising large variably PCNA immunostained type A spermatogonia (sg), and two somatic cell types, namely large PCNA-negative irregular shaped to oblong cells (filled arrows), and small immunostained ovoid to fusiform cells (open arrows). The latter's arrangement in parallel rows indicate the early stages of the assembly of a collecting duct. Immunostained fusiform somatic cells (fu) are also closely aligned to several type A spermatogonia. Bar = 20 μm.

53x30mm (600 x 600 DPI)

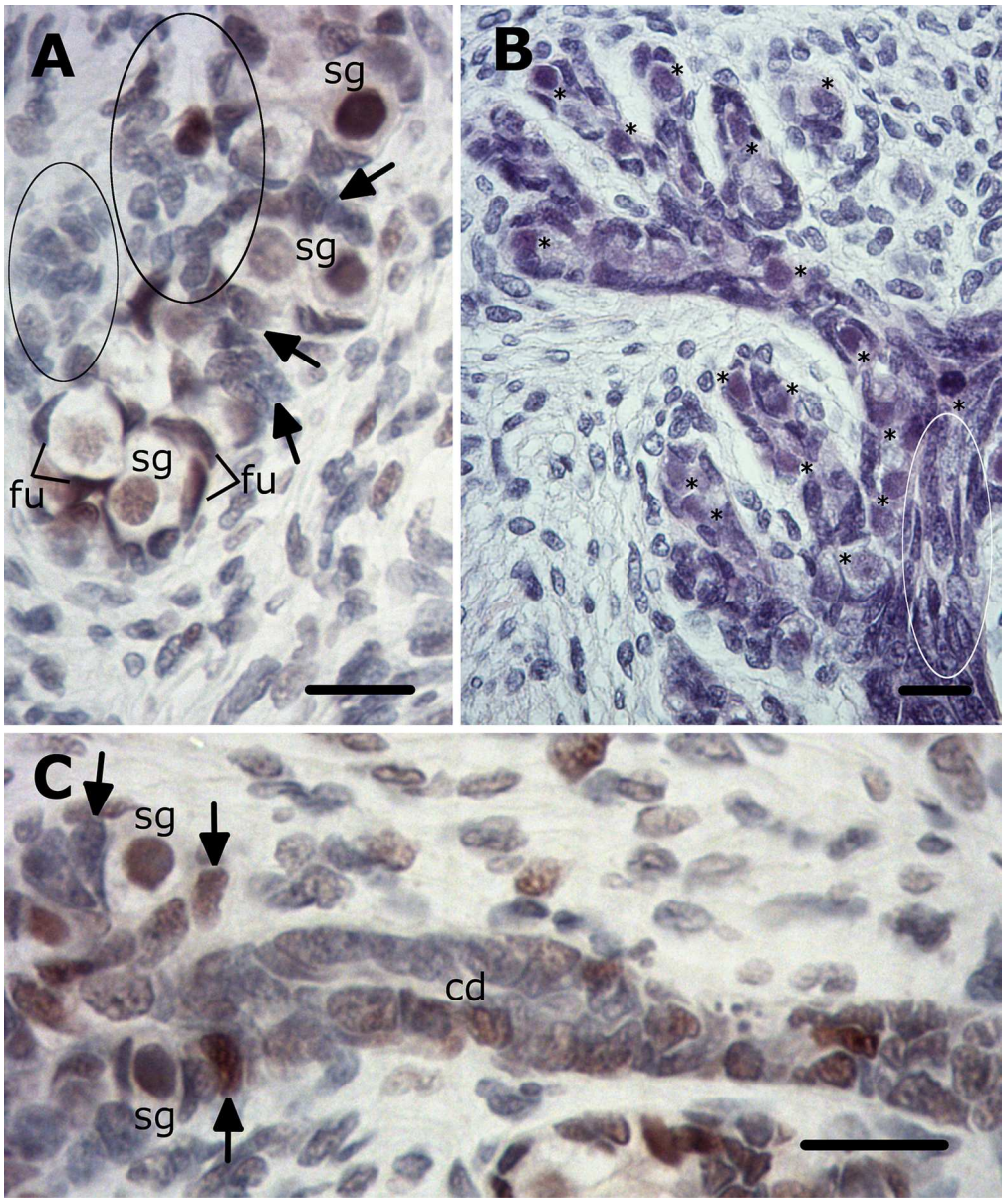

Figure 3. Pre-spermatogenesis is associated with a rearrangement of the soma – germ line relationships in the germinal ridge (GR) of *P. glauca*. (A) Large irregular shaped to oblong stromal cells (filled arrows) aggregate around (black circled areas) and amongst small groups of A-spermatogonia (sg), some of which visibly lack an accompanying fusiform supporting cell (fu) and are instead surrounded by the former somatic cell type (filled arrows). (B) A hematoxylin and eosin-stained section showing a region of the GR and the development of branching cords comprising the large irregular shaped to oblong stromal cells (white circled area). The spermatogonia (asterisks), that are scattered along the cords also demarcate the limits of the cord branches (C) A further development shows the assembly of a decidedly thick collecting duct (cd) from the latter somatic cell type (filled arrows). Bar = 20 μm.

72x86mm (600 x 600 DPI)

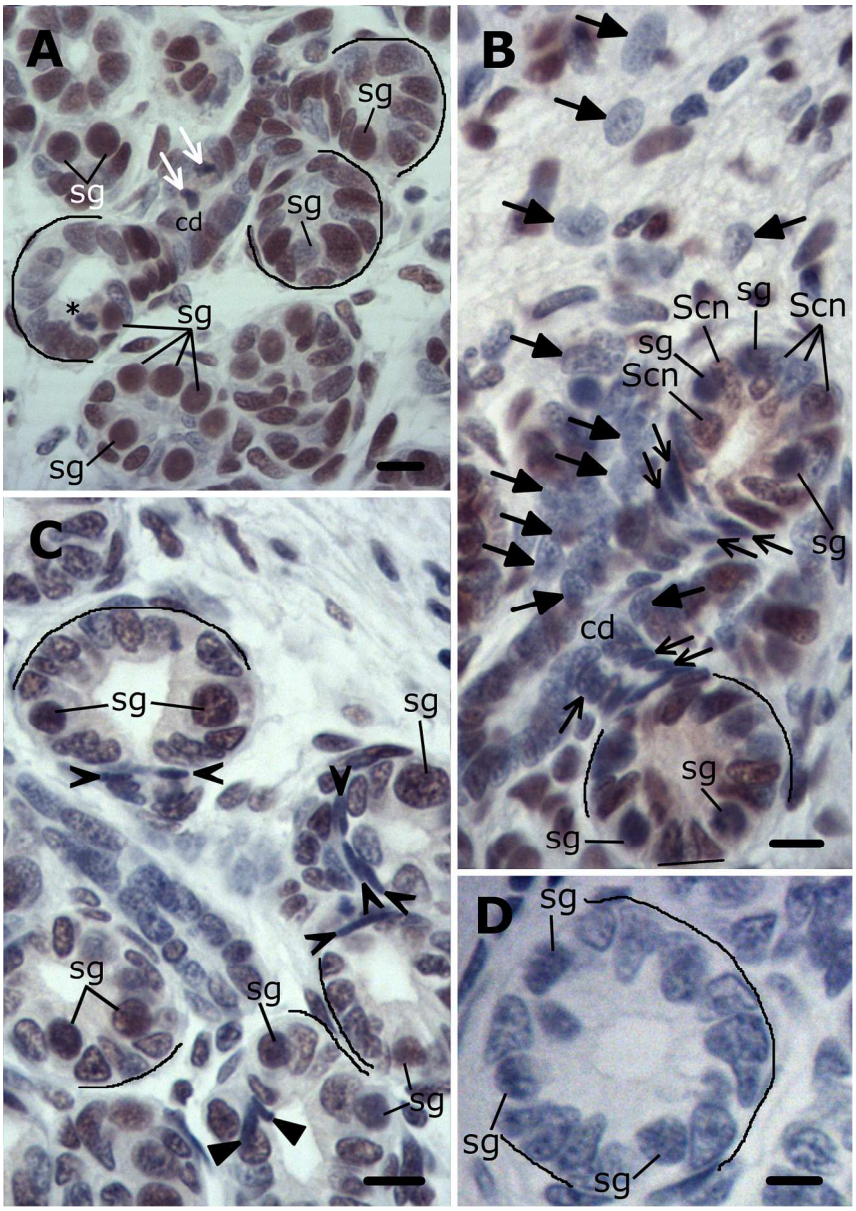

Figure 4. The developing testicular parenchyma in the germinal zone of adult *P. glauca* is initially more tubular-like than cyst-like. (A) The appearance of large oblong stromal-derived cells arranged in open ended rings, housing a single isolated spermatogonium (sg), at the termini of the lengthening collecting duct (cd) identify the rings as the early cysts and the oblong cells as the Sertoli cells (underlined). (B, C) Growth of the collecting ducts is also due to the incorporation of large oblong stromal cells (black filled arrows) that aggregate around the ducts. The duct cells nearest to the cyst opening become gradually ovoid to elongated (black open arrows). The duct cells bordering on the Sertoli cells that demarcate the cyst opening are strongly basophilic slender elongated cells (arrowheads). The latter seal the cyst opening, and may take up positions among the Sertoli cells (filled arrowheads). Note the consistent absence of Sertoli cell mitotic figures. (D). A negative control section that shows a Sertoli cell-dominated cyst with a few basophilic spermatogonia (sg) and Sertoli cells that display bulky oblong nuclei (underlined). Mitotically active duct cells (white open arrows), spermatogonial mitosis (black asterisk). Bar (A, B, C) = 10 μm, D = 5 μm.

80x114mm (600 x 600 DPI)

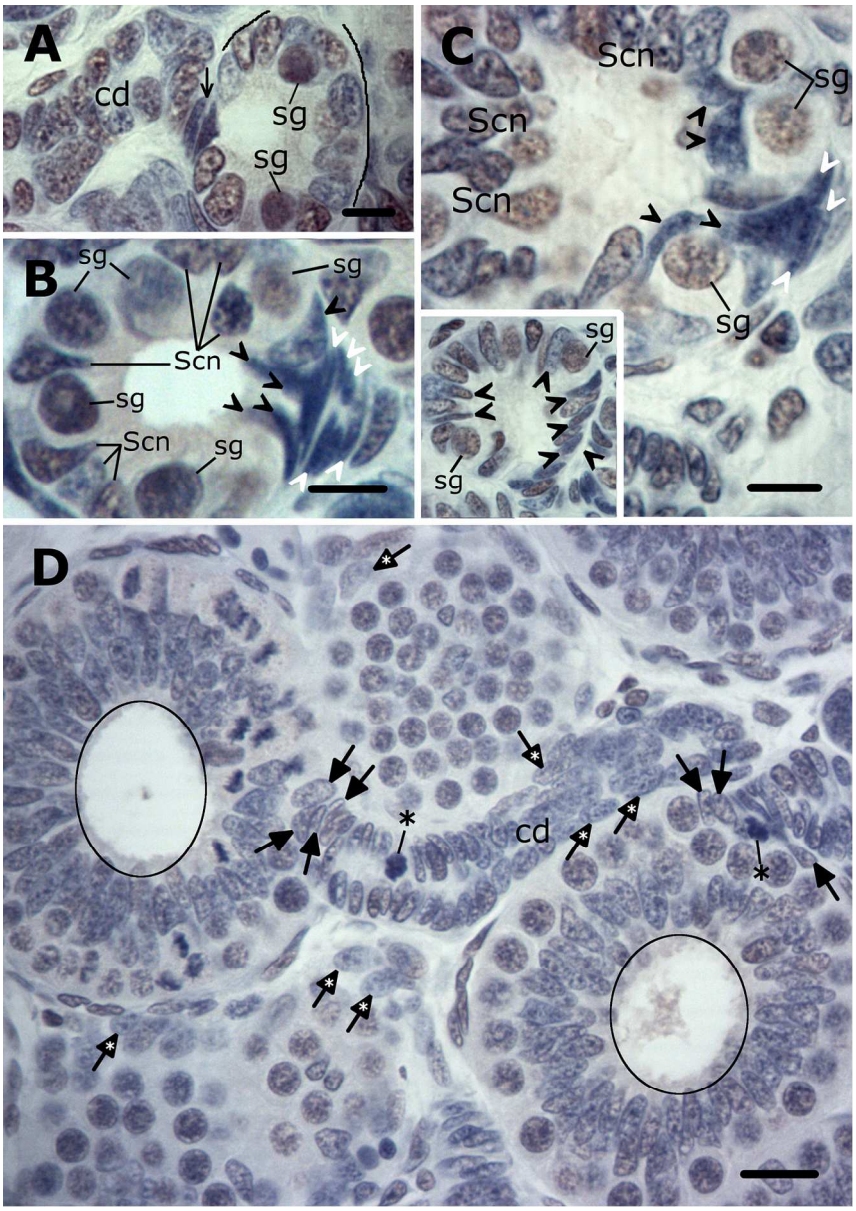

Figure 5. The two types of duct – cyst transitions observed in developing *P. glauca* spermatogonial cysts with Sertoli cells that possess large oblong nuclei (underlined, Scn). (A) A suitable plane of sectioning through a newly formed cyst shows the one type of duct – cyst transition, during which the cyst opening is sealed by slender, spindle-shaped basophilic cells (open arrows) and reinforced by large duct cells. (B) The duct – cyst interface in other cysts show the generation of extremely slender spindle-like basophilic cells (white arrowheads) that undergo a gradual transformation (black arrowheads) simultaneously as their long axes are increasingly reoriented perpendicular to the cyst periphery. (C) A tangentially sectioned cyst showing that the slender, transforming basophilic cells (black arrowheads) may aggregate in between the oblong Sertoli cell nuclei (Scn) and curve around the spermatogonia (sg) on their luminal sides, all indicative of the appearance of an atypical Sertoli cell type. Inset: A newly formed Sertoli cell-dominated cyst with several slender atypical Sertoli cells (black arrowheads) interspersed among the large oblong Sertoli cells. (D) In other spermatogonial cysts with large oblong Sertoli cells, such as these two patterned cysts with perilumenar Sertoli nuclei (underlined), duct cell mitotic activity (black asterisk) in the neck region and duct

– cyst interface causes the displacement of duct cells (filled arrows) into the cysts. Notes that the cyst's Sertoli cell population is also experiencing a wave of mitosis. The duct neck region is distinct from the primary collecting duct (cd) that consists of broad oblong cells (asterisk-labeled filled arrows) found scattered in the interstitium. Bar = (A, B, C) = 10 µm, D = 20 µm.

77x109mm (600 x 600 DPI)

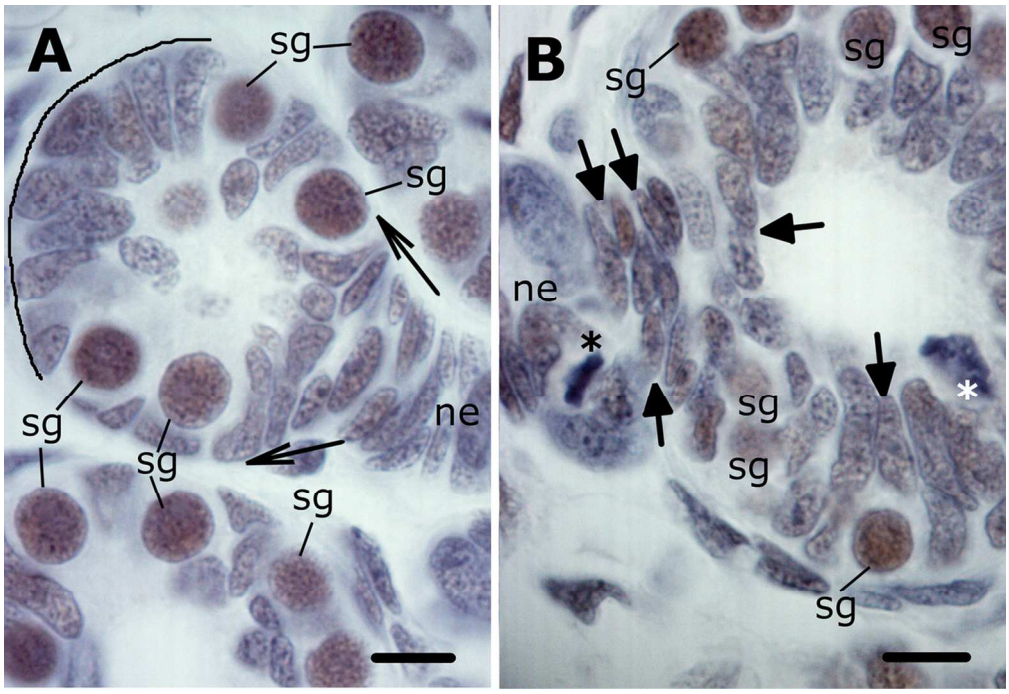

Figure 6. Some spermatogonial cysts of *P. glauca* house Sertoli cells whose nuclei have irregular, often elongated profiles and pointed ends. (A) The cyst's Sertoli cell complement (underlined) is supplemented by similar-looking duct cells (long arrows) migrating in from the neck region (ne). (B) A deeper plane of sectioning through a larger cyst reveals a dynamic duct – cyst transition area and the continued displacement of elongated duct cells into the cyst (filled arrows). Note the markedly different quality of immunostaining and architecture of the spermatogonial nuclei (sg). Duct and Sertoli cell mitoses (black and white asterisks), respectively. Bar = 10 μm.

55x37mm (600 x 600 DPI)

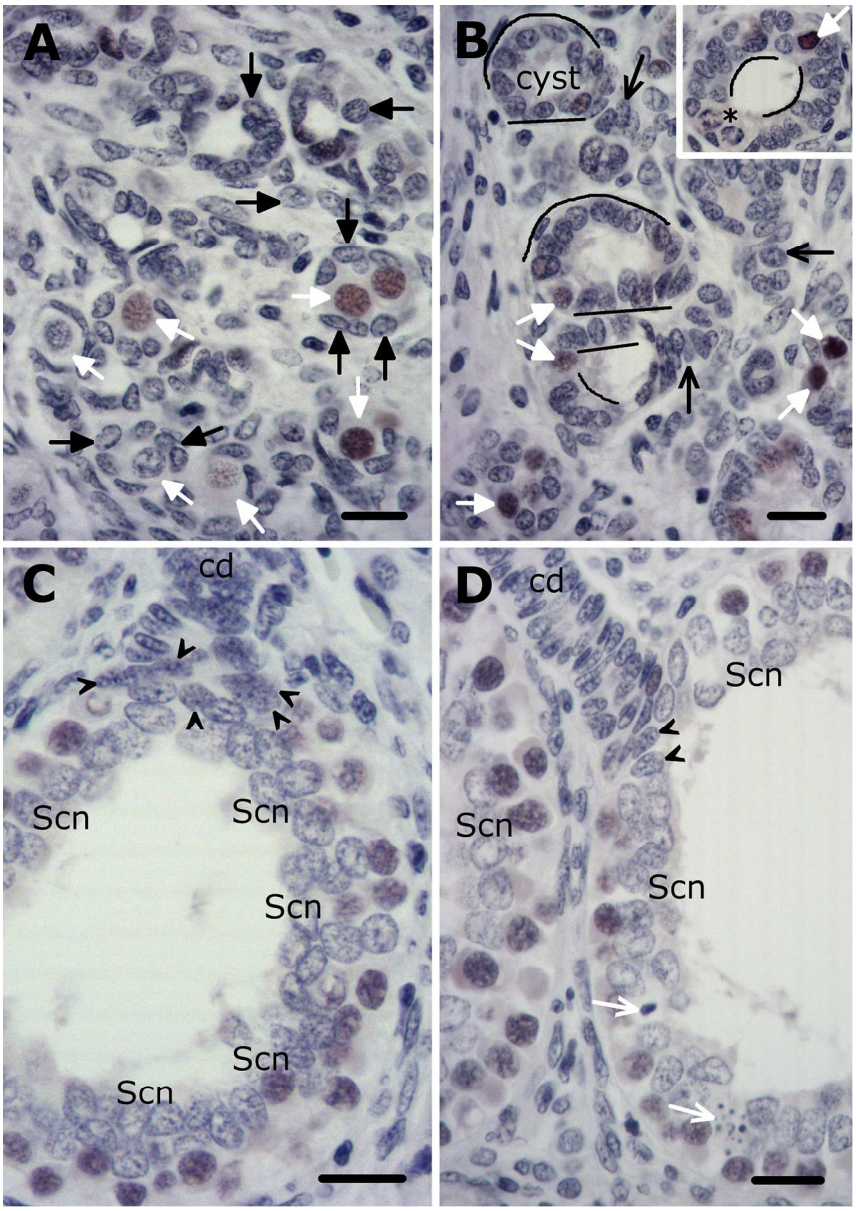

Figure 7. The duct – cyst relationship in newly formed and growing spermatogonial cysts in *I. oxyrinchus*. (A) Large spherical and frequently PCNA-positive A-spermatogonia (white filled arrows) are seen scattered among ovoid to oblong cells (black filled arrows) that comprise the homogeneous stromal tissue in this species. (B) The ring shaped arrangement of stromal cells, some of whom are weakly PCNA immunoreactive, alongside a lone moderate to strong PCNA immunostained spermatogonium (white filled arrows) definitively identifies these structures as cysts and the stromal-like cells as the Sertoli cells (underlined). Note that the assembly of the cyst takes precedence over that of the collecting duct (black open arrows). Inset: Occasionally observed mitotic figures (asterisk) in an otherwise Sertoli cell-dominated (underlined) cyst are those of dividing spermatogonia. (C) The duct – cyst transition area in larger patterned spermatogonial cysts shows an accumulation of duct cells with noticeably cloudy nuclei, some of which are displaced (arrowheads) towards the pale bulky Sertoli cell nuclei (Scn) that line the cyst lumen. (D) The inward displacement of duct cells (arrowheads) that supplement the Sertoli cell population (Scn) gradually declines with subsequent growth of the spermatogonial cyst. Note the presence of pyknotic bodies in this cyst (white open arrows)

that result from spermatogonial death. Bar = 20 μm.

76x107mm (600 x 600 DPI)

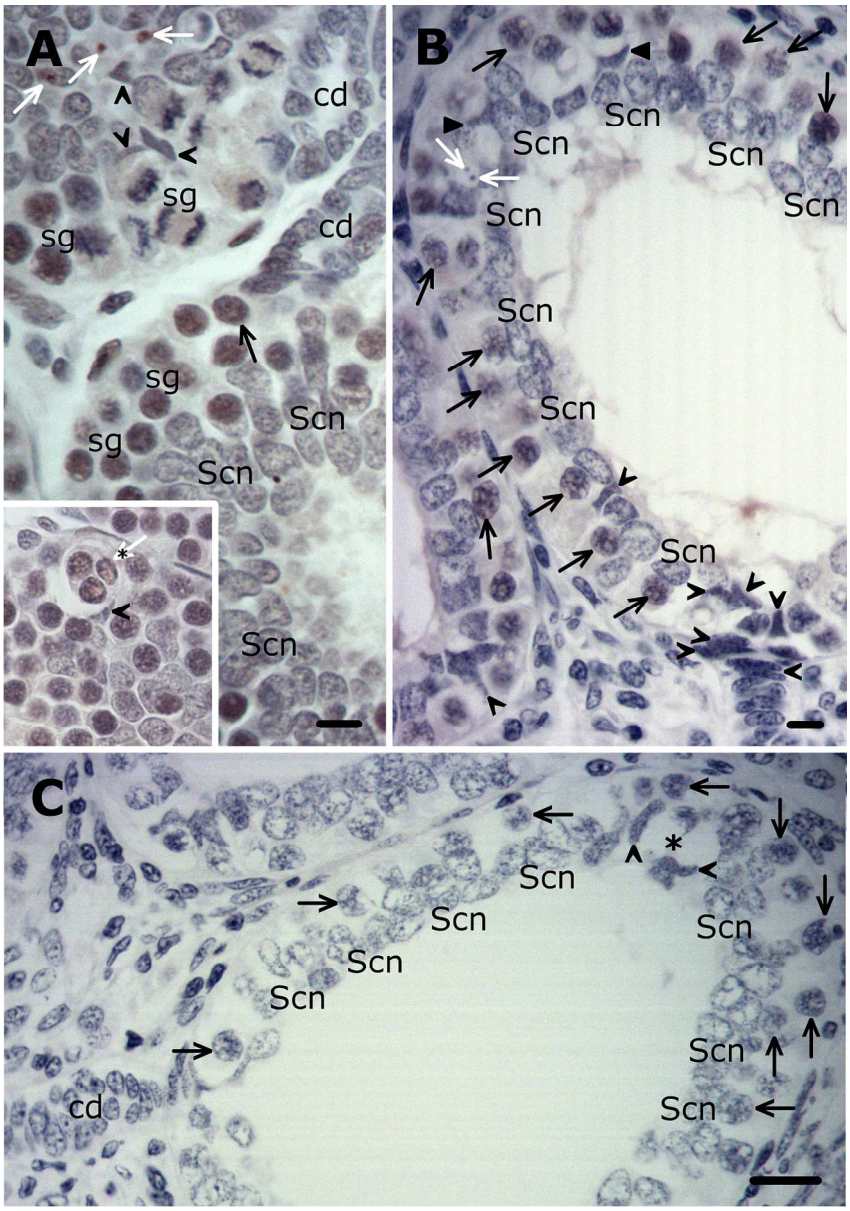

Figure 8. In both (A) *P. glauca* and (B, C) *I. oxyrinchus*, some developing patterned spermatogonial cysts may reveal the atypical Sertoli cell with its basophilic elongated to fusiform nucleus. (A) These atypical Sertoli cells (open arrowheads) are observed in close proximity to dividing B-spermatogonia (sg) and cell debris (white arrows). Inset: Such a Sertoli cell is sometimes seen tightly apposed to spermatogonia undergoing multinucleate cell death (asterisk-labelled white arrow) in mature patterned cysts further downstream in the spermatogenic sequence. (B) A comparable *I. oxyrinchus* cyst likewise shows these small dark Sertoli cells in proximity to vacuolated areas (filled arrowheads) that may or may not reveal pyknotic bodies (white arrows). Note the aggregation of the small dark Sertoli cells at the duct – cyst interface. (C) Negative control of cross section adjacent to that shown in (B). The large vacuolated area (asterisk) in the spermatogonial layer is bordered by two atypical Sertoli cells. Bar (A, B) = 10 μm, C = 20 μm.

166x236mm (300 x 300 DPI)

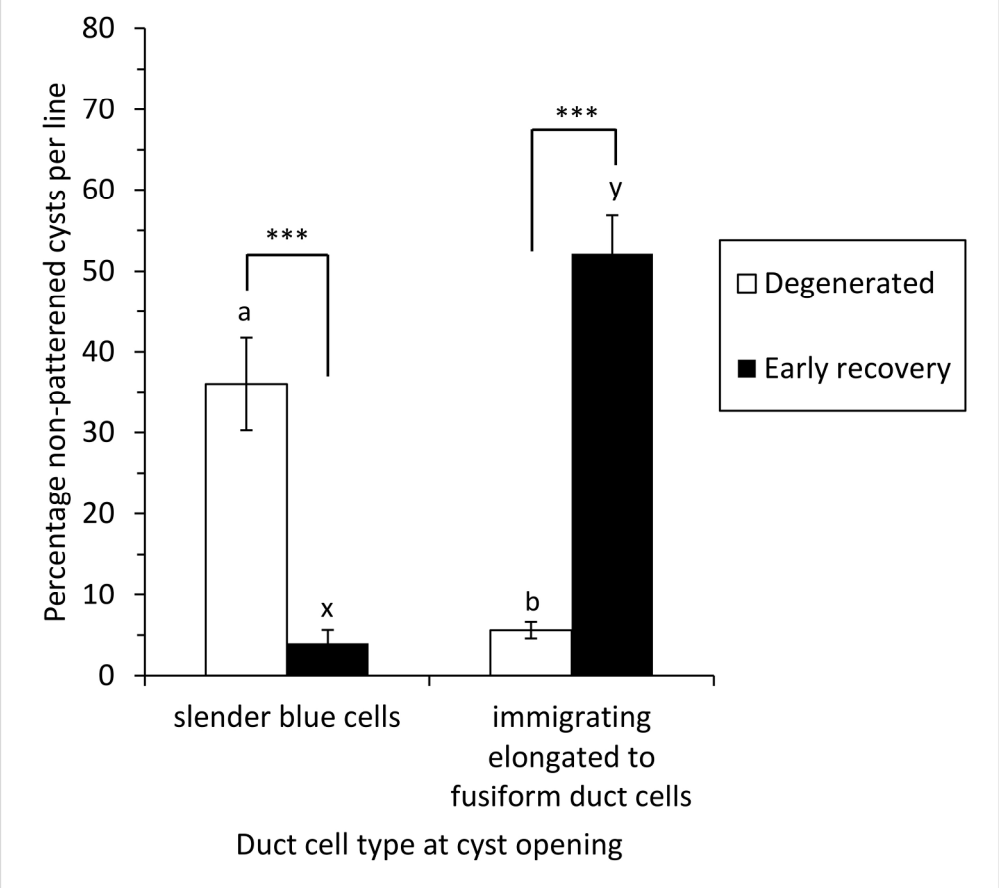

Figure 9. Percentages of non-patterned cysts that show differences in the type of immigrating duct cell at the cyst opening, expressed as a function of testicular condition in wild-caught *P. glauca* specimens (n = 10). Values represent the mean percentage ± S.E.M non-patterned cysts analyzed by one-way ANOVA. The Student Newman-Keuls multiple comparison test was used to identify mean percentages that differed significantly. Different letters and asterisks indicate significant differences ($P < 0.001$).

106x94mm (600 x 600 DPI)

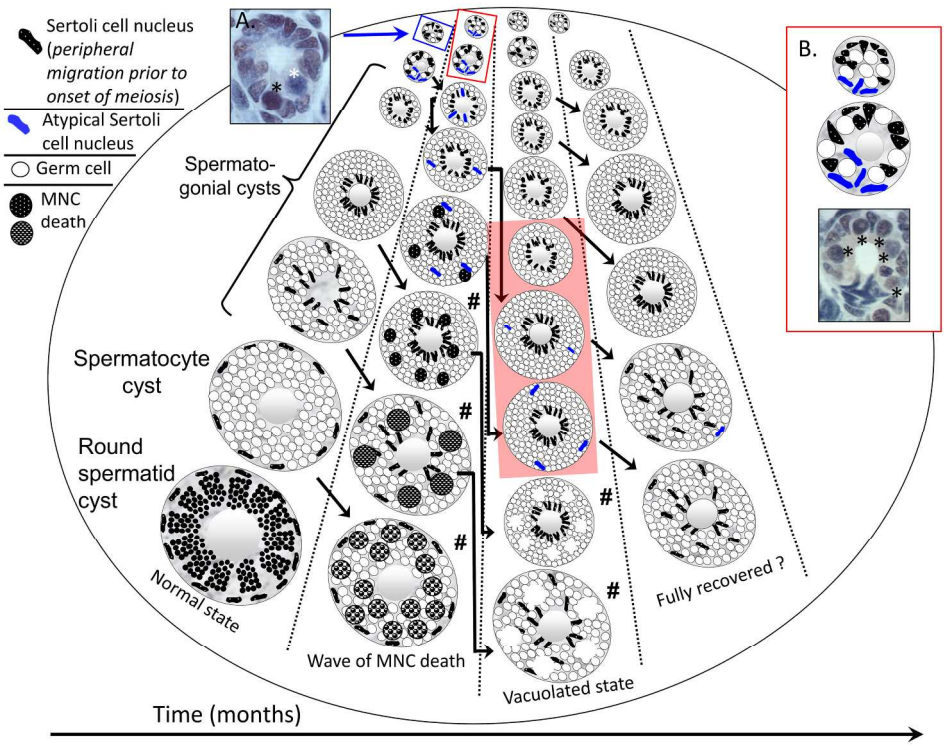

Figure 10. A schematic representation, based on previous quantitative analyses (McClusky, 2011, 2013), that sketches the putative involvement of the small atypical Sertoli cell in successive spatiotemporal changes of cyst stages (mainly spermatogonial and spermatocyte cysts) that readily reveal the onset of the wave of multinucleate cell (MNC) death and vacuolated areas in testicular cross-sections of summer-breeding *P. glauca*. Each column of cysts portrays a snapshot of the relevant spermatogonial and spermatocyte cysts found in a single cross-section of the testes from specimens whose cyst compositions were relatively similar, all of which facilitated the extrapolation of the developmental advance of these cyst stages, and the onset and progression of the wave of MNC death in the latter cyst stages (squares) forwards and backwards in time. As discussed previously (McClusky, 2013), the vacuolated appearance in indicated cyst stages is evidence of the Sertoli cell's phagocytic removal of the earlier formed MNC corpses (squares). The significant quantitative correlation between immature spermatogonial cysts that reveal the small atypical Sertoli cells and the degenerated testicular condition (wave of MNC death) reported in Fig. 9 are related to two phenomena manifested in affected cysts. The first phenomenon is the limitation of the spread of MNC wave of death in these immature spermatogonial cysts that contain some atypical Sertoli cells (i.e. a spatial effect) that in turn corresponds in time with a second phenomenon, namely the latter's normal developmental advance to the mature spermatogonial cyst stage (red-shaded area) during the early recovery or vacuolated appearance phase (i.e. a temporal effect), all of which in turn may explain the full recovery of the testis in this highly seasonal species. This rationale follows previously reported (McClusky, 2011) quantitative analyses which showed a lower and higher fraction of degenerated spermatogonial and spermatid cysts, respectively, in the vacuolated testicular state compared to those cysts in the MNC affected testes. In other words, the effects of the wave of MNC death are evident in subsequent cyst stages in the early recovery phase, with no new degenerated phenomena arising in the recovering testis. Insets A and B show the typical PCNA immunostaining patterns of newly assembled cysts in the GZ that may either lack (A) or reveal (B) the appearance of these highly recognizable blue atypical Sertoli cells. Note that spermatogonia in these Sertoli cell-dominating cysts are characteristically either PCNA-negative (quiescent, white asterisk) or may reveal intense homogeneously or variable brown immunostaining (black asterisks).

109x82mm (600 x 600 DPI)